Physica B 449 (2014) 155–159

Contents lists available at ScienceDirect

Physica B

journal homepage: www.elsevier.com/locate/physb

Structural and calorimetric studies of two crystallization stages of $Ag_{10}As_{30}S_{60}$ glassy alloys

M.I. Abd-Elrahman [a,*], Rasha M. Khafagy [b], Noha Younis [a], M.M. Hafiz [a]

[a] Physics Department, Faculty of Science, Assiut University, Assiut 71516, Egypt
[b] Materials Science Laboratory, Physics Department, Girls College for Arts, Science, and Education, Ain Shams University, Cairo, Egypt

ARTICLE INFO

Article history:
Received 15 April 2014
Received in revised form
14 May 2014
Accepted 17 May 2014
Available online 23 May 2014

Keywords:
Chalcogenide
Structural characterization
Thermal analyses
Crystallization kinetics

ABSTRACT

The structure of the as-prepared and thermal annealed $Ag_{10}As_{30}S_{60}$ chalcogenide glass is characterized using the X-ray diffraction (XRD) and scanning electron microscopy (SEM). Differential scanning calorimetry (DSC) curves recorded at four different heating rates are analyzed to determine the glass and crystallization transition temperatures, thermal stability and enthalpy release. Two separated crystallization peaks are observed in the DSC curves. XRD results indicate the precipitation of $AgAsS_4$ crystal phase is responsible for the first peak. Numerous phases with S_8 dominant phase are accountable for the second peak. The crystallization kinetics such as the activation energy for the crystallization (E_c), the frequency factor (K_o) and the crystallization rate constant K are determined for each crystallization stage. The results show that the crystallization rate constant for the first crystallization stage is about six times larger than that of the second crystallization step.

1. Introduction

The metallic chalcogenide glasses are suitable materials for optical memories because amorphous or crystalline state is reachable due to high structural flexibility employing weakly bonding "lone pair" p-electrons [1]. They have received much attention due to their potential applications in thermoelectric, electronic, and optical devices [2]. Binary As–S alloys can be formed with an As content up to 46%, however glasses with low As content can easily crystallize [3]. Addition of silver (Ag) with ionic nature results in various structural changes in the materials which in turn modify the band structure and hence electrical properties of the material. Chalcogenide containing Ag found applications in optical memory material [4,5].

Many investigators have studied the formation of homogeneous binary and ternary phases after the doping of Ag in As–S [6–10]. They have tried to explain the mechanism of silver doping and the structure of chalcogenide glasses. The phase diagram of ternary $Ag_x(As_{33}S_{67})_{100-x}$ relating between phases and temperature had showed two regions where homogeneous glass formation occurs: $x=0$ (AsS_2) and $x=25$ ($AgAsS_2$) [11]. Crystalline forms of the silver sulfarsenide $AgAsS_2$ occur in nature as monoclinic [12] and rhombohedral [13]. Understanding the structural and thermal properties of Ag–As–S glass requires a detailed knowledge of its crystalline phases and crystallization kinetics.

Since the crystallization of a chalcogenide glass is a highly exothermic process, differential scanning calorimetry (DSC) is a suitable technique for obtaining the parameters of crystallization kinetics, such as the activation energy for the crystallization (E_c), the frequency factor (K_o) and the crystallization rate constant K [14,15]. In calorimetric measurements, two basic methods, isothermal and non-isothermal are used. In the non-isothermal measurements, the sample is heated at a fixed rate and the heat evolved is recorded as a function of temperature. From the heating rate dependence of peak crystallization temperature (T_p), the activation energy for crystallization can be calculated [16].

The aim of this work is to study the crystallization kinetics of the $Ag_{10}As_{30}S_{60}$ chalcogenide glass which has two stages of crystallizations by DSC technique under non-isothermal conditions. The characteristic parameters such as thermal stability and enthalpy are also computed from the heating rate dependence of the crystallization phase transition.

2. Experimental

Bulk $Ag_{30}As_{10}S_{60}$ material was prepared using the well known melt-quench technique. In this technique, purity (99.99%) of Ag, As and S (from Aldrich Co., UK) in atomic proportions was weighed in a quartz glass ampoule (12 mm diameter). The ampoule containing

* Corresponding author. Tel.: +201092808520; fax: +20882342708.
E-mail address: mostafaia11@yahoo.com (M.I. Abd-Elrahman).

http://dx.doi.org/10.1016/j.physb.2014.05.028
0921-4526/

15 g total was sealed in a vacuum of 10^{-4} Torr and heated in a rotating furnace at around 900 °C for 20 h. The ampoule was then quenched in ice-cold water.

In order to study the effect of the thermal annealing on the structure, some samples were annealed at different temperatures which were 500 and 573 K for 1.0 h. To identify the amorphous state and the induced crystallization phases due the thermal annealing process, X-ray investigation of the as-prepared and the annealed samples is performed using a Philips diffractometer, PW1710, Netherlands, with Ni filtered Cu$K\alpha$ source (λ=0.154 nm). A Scanning Electron Microscopy (SEM) apparatus, Jeol (JSM)-T200 type-Japan, was used to investigate the surface morphology of the as-prepared and thermally annealed samples. The thermal behavior was investigated using a DU Pont 1090 differential scanning calorimeter (DSC). The temperature and energy calibrations of the instrument are performed using the well-known melting temperature and melting enthalpy of high-purity indium supplied with the instrument. The calorimetric sensitivity was 10 μW/cm and the temperature precision was ±0.1 K. The sample was heated in nitrogen atmosphere under non-isothermal conditions at different heating rates (5–20 K/min).

3. Results and discussion

3.1. X-ray diffraction

The X-ray diffraction (XRD) patterns of the as-prepared $Ag_{10}As_{30}S_{60}$ alloy and those annealed at 500 and 573 K for 1 h are shown in Fig. 1. It can be noticed that the XRD of the as-prepared sample has no any sharp peak indicating the typical amorphous state of the synthesized composition. To examine the effect of the thermal annealing on the structural properties, some samples are annealed at temperatures 500 and 573 K. The chosen of these temperatures are based on the DSC feature of the alloy as it will be discussed herein after. That is, the thermal annealing at each temperature of them causes a stage of crystallization.

The X-ray examination of the 500 K annealed sample (Fig. 1) shows that the sample is crystallized in preferential orientation indicated with strong peak. This orientation is along (0 2 0) plane corresponding the ternary $AgAsS_4$ phase. The association of the phases are determined on the basis of best agreement between observed of 2θ and inter-planar spacing, $d_{exp.}$, with those of American Society for Testing and Materials (ASTM), $d_{stand,}$ as presented in Table 1. For the sample annealed at 573 K, many diffraction patterns are observed indicating numerous crystallite phases. Strong peaks indicate preferential orientations of the crystallized sample. These orientations are

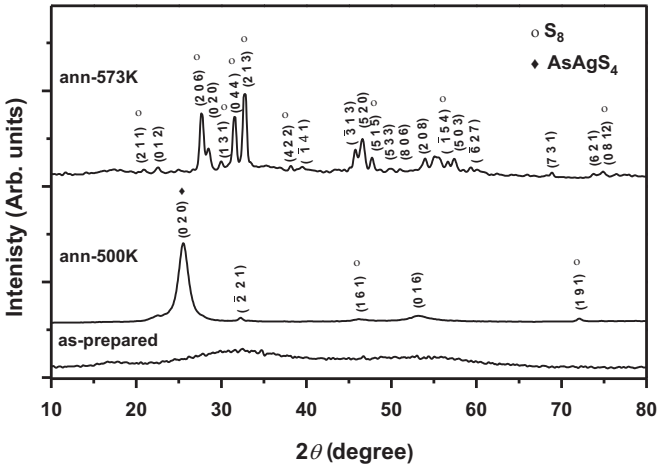

Fig. 1. X-ray diffraction pattern of $Ag_{10}As_{30}S_{60}$ alloy for as-prepared and after annealing at two different temperatures for 1 h.

Table 1
Measured and standard ASTM values for diffrograms and calculated particle size (D) for the bulk of $Ag_{10}As_{30}S_{60}$ alloy.

Annealed Temp. (K)	$2\theta_{exp}$ (degrees)	$2\theta_{stand}$ (degrees)	$d_{exp.}$ (Å)	d_{stand} (Å)	$h\,k\,l$	Phase	D (nm)
500	22.54	22.54	3.941	3.941	0 1 2	$AsAg_3S_3$	16.97
	25.54	25.54	3.485	3.485	0 2 0	$AsAgS_4$	6.16
	32.273	32.243	2.772	2.774	$\bar{2}$ 2 1	$AsAg_3S_3$	13.25
	46.18	46.19	1.964	1.963	1 6 1	S_8	13.30
	53.14	53.14	1.722	1.722	0 1 6	$Ag_7S_2(AsS_4)$	3.92
	72.1	72.1	1.309	1.309	1 9 1	S_8	14.66
573	20.86	20.81	4.26	4.265	2 1 1	S_8	11.02
	22.54	22.538	3.941	3.941	0 1 2	$AsAg_3S_3$	12.87
	27.69	27.69	3.218	3.218	2 0 6	S_8	11.63
	28.48	28.48	3.131	3.131	0 2 0	$AsAg_3S_3$	15.19
	29.98	29.96	2.978	2.979	1 3 1	S_8	13.53
	31.556	31.6	2.833	2.826	0 4 4	S_8	12.03
	32.75	32.74	2.731	2.733	2 1 3	S_8	11.39
	38.14	38.11	2.358	2.359	4 2 2	S_8	14.81
	39.52	39.51	2.27	2.279	$\bar{1}$ 4 1	As_4S_4	13.06
	45.76	45.79	1.981	1.98	$\bar{3}$ 1 3	AsS	21.82
	46.6	46.65	1.947	1.945	5 2 0	$Ag_7S_2(AsS_4)$	12.69
	47.74	47.74	1.904	1.903	5 1 5	S_8	14.51
	49.9	49.9	1.826	1.826	5 3 3	$AsAgS_2$	4.65
	50.98	50.98	1.79	1.789	8 0 6	$AsAgS_2$	19.43
	53.98	53.95	1.697	1.698	2 0 8	$AsAg_3S_3$	15.80
	56.62	56.624	1.624	1.624	$\bar{1}$ 5 4	S_8	16.66
	57.4	57.41	1.604	1.604	5 0 3	As_4S_3	11.44
	59.32	59.32	1.557	1.557	$\bar{6}$ 2 7	$AsAg_3S_3$	14.42
	68.86	68.8	1.362	1.363	7 3 1	$Ag_7S_2(AsS_4)$	19.90
	73.78	73.80	1.283	1.283	6 2 1	$AsAg_3S_3$	25.68
	74.86	74.841	1.267	1.267	0 8 12	S_8	19.86

along (2 0 6), (0 4 4) and (2 1 3) planes corresponding S_8 phase. In addition, the peak of $AgAsS_4$ phase is faded away in the case of the 573 K annealed sample. In general, the diffraction patterns in the case of 573 K annealed sample have different positions from those appeared in the XRD of the 500 K annealed sample. These observations indicate existence of another crystallization stage.

The grain size (D) for the crystallites are calculated from positions and widths of the peaks using the well known Scherer's formula

$$D = \frac{0.94\lambda}{\beta \cos \theta}, \tag{1}$$

where λ in nm is the X-ray wavelength, β in radian is the broadening of the diffraction peak and θ is the diffraction angle in radian. The D values are calculated from the diffraction peaks and collected in Table 1. The averages of grain size are found to be 11.3 and 14.9 nm for the first and second crystallization stages, respectively.

3.2. Surface morphology

Fig. 2 shows the SEM micrographs of the as-prepared $Ag_{10}As_{30}S_{60}$ alloy and those annealed at 500 and 573 K. Fig. 2a shows the SEM image of a fractured, as prepared, bulk specimen of $Ag_{10}As_{30}S_{60}$ alloy indicating the amorphous structure of the investigated sample. This observation of the amorphous structure is confirmed in the XRD (Fig. 1). Fig. 2b and c show comparative images for the aggregation of the crystallite particles and their sizes after annealing at two different temperatures. The micrograph of the annealed sample, at 500 K (Fig. 2b), shows the existence of a polycrystalline structure consisting of crystallites embedded in amorphous phase. The scanning electron micrograph for the annealed $Ag_{30}As_{10}S_{60}$ alloy at 573 K is shown in Fig. 2c. A polycrystalline structure consisting of different crystalline phases embedded in an amorphous matrix is observed. Some of these crystallized particles are interconnected and others are isolated. However, the grain size is larger for 573 K annealed bulk than that of 500 K.